



# Magnesia-supported gold nanoparticles as efficient catalysts for oxidative esterification of aldehydes or alcohols with methanol to methyl esters

Xiaoyue Wan, Weiping Deng\*, Qinghong Zhang, Ye Wang\*

State Key Laboratory of Physical Chemistry of Solid Surfaces, Collaborative Innovation Center of Chemistry for Energy Materials, National Engineering Laboratory for Green Chemical Productions of Alcohols, Ethers and Esters, College of Chemistry and Chemical Engineering, Xiamen University, Xiamen 361005, China

## ARTICLE INFO

### Article history:

Received 9 October 2013

Received in revised form

23 November 2013

Accepted 2 December 2013

Available online xxx

### Keywords:

Oxidative esterification

Gold nanoparticles

Magnesia

Bifunctional catalyst

Methacrolein

Methyl methacrylate

## ABSTRACT

Magnesia-supported gold nanoparticles were found to be highly efficient catalysts for the oxidative esterification of methacrolein (MAL) with methanol in the presence of molecular oxygen into methyl methacrylate (MMA) under liquid base-free conditions. MAL conversion of 98% and MMA selectivity of 99% were obtained over the Au/MgO catalyst at 343 K after a 2 h reaction. Besides the Au nanoparticles, the support also played pivotal roles in the oxidative esterification of MAL. The support with higher density of basic sites, particularly stronger basic sites, showed better performances for the formation of MMA. The enhancement of the intermediate formation by the basic sites is proposed to be the key reason for the superior activity of the Au/MgO catalyst. Our studies on the size effect of Au nanoparticles reveal that smaller Au nanoparticles favor the transformation of MAL, and the turnover frequency increases with decreasing mean size of Au nanoparticles. This suggests that the Au-catalyzed oxidative esterification of MAL is a structure-sensitive reaction. We have demonstrated that the Au/MgO catalyst is also applicable to the oxidative esterification of different aldehydes and alcohols.

© 2013 Elsevier B.V. All rights reserved.

## 1. Introduction

Methyl methacrylate (MMA) is an important chemical, which is widely used for producing acrylic plastics (polymethyl methacrylate) or polymer dispersions for paints and coatings [1,2]. Currently, MMA is mainly produced by the acetone cyan hydrine (ACH) method [1,2]. However, this process suffers from the problems of using highly toxic hydrogen cyanide as the raw material and handling the resulting ammonium sulfide waste [2]. Therefore, many efforts have been devoted to developing environmentally benign alternatives for the production of MMA. The oxidative esterification of methacrolein (MAL) with methanol in the presence of O<sub>2</sub> is one of the most attractive routes for the production of MMA (**Scheme 1**).

Supported Pd catalysts have been reported to be efficient for the direct oxidative esterification of MAL and other aldehydes or alcohols with methanol to the corresponding esters [2–6]. However, the selectivity of MMA is typically low over supported Pd catalysts. The modification of Pd catalysts by Pb forming Pd<sub>3</sub>Pb phase could

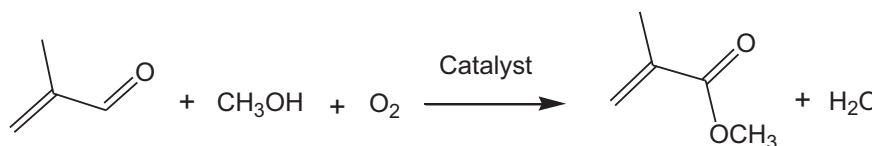
improve the selectivity of MMA [2], but Pb is quite toxic. Furthermore, the use of liquid base additives is required for the Pd-based catalysts.

On the other hand, Au catalysts have attracted considerable interest because of their unique catalytic behaviors, especially unique selectivity in many reactions [7–11]. Generally, the catalytic behavior of supported Au catalysts depends on the size and chemical state of Au particles, the property of the support, and the Au-support interaction. Au-based catalysts have been successfully used for the direct oxidative esterification of primary alcohols with methanol to methyl esters [12–24]. A wide range of materials such as Al<sub>2</sub>O<sub>3</sub> [12], TiO<sub>2</sub> [13–15], CeO<sub>2</sub> [16–18], Ga<sub>2</sub>O<sub>3</sub> [19], SiO<sub>2</sub> [20–22], polymers [23], and hydrotalcite [24] have been exploited as supports of Au catalysts for these reactions. However, in most cases, a liquid base additive, e.g., alkali carbonate (K<sub>2</sub>CO<sub>3</sub>, Na<sub>2</sub>CO<sub>3</sub>), alkali hydroxide (NaOH, KOH), or NaOCH<sub>3</sub> is required to achieve high yields of the target ester [16,18,19,24]. This makes the process less green and less cost-effective.

Recently, we have aimed at developing efficient Au catalysts capable of working for the oxidative esterification of MAL with methanol to MMA in the absence of any liquid bases. Here, we report our finding that Au nanoparticles loaded on a solid base, i.e., MgO, are highly efficient catalysts for liquid base-free oxidative esterification reactions. The effects of the support and the Au

\* Corresponding authors. Tel.: +86 592 2186156; fax: +86 592 2183047.

E-mail addresses: [dengwp@xmu.edu.cn](mailto:dengwp@xmu.edu.cn) (W. Deng), [\(Y. Wang\)](mailto:wangye@xmu.edu.cn).



**Scheme 1.** Oxidative esterification of methacrolein with methanol to methyl methacrylate.

particle size will be discussed in detail. The substrate scope of the Au/MgO catalyst will also be investigated.

## 2. Experimental

### 2.1. Catalyst preparation

The supported Au catalysts were prepared by a deposition–precipitation (DP) method using urea as a homogeneous precipitant. In brief, urea was first added into an aqueous solution of HAuCl<sub>4</sub> (typically 0.48 mmol L<sup>-1</sup>) with a molar ratio of urea/Au of 100:1. Then, the support was added into the mixed aqueous solution, and the suspension was vigorously stirred at 353 K. After aging for a certain time (typically 4 h), the solid product was recovered by centrifugation followed by thorough washing with deionized water to remove the remaining chloride anion. The resulting powdery solid was dried in air at 353 K for 1 h, and finally reduced in H<sub>2</sub> at 523 K for 2 h. The concentration of HAuCl<sub>4</sub> and the aging time were regulated to control the size of Au nanoparticles as reported previously [25]. The target Au loading in each catalyst used in this work was 0.5 wt%.

### 2.2. Catalyst characterization

Transmission electron microscopy measurements were carried out on a JEM-2100 electron microscope operated at an acceleration voltage of 200 kV. The mean size of Au nanoparticles in the sample was estimated from the TEM micrographs by counting around 150–200 particles. By assuming a spherical model of Au nanoparticles, the Au dispersion (*D*) could be estimated by using the following relationship, *D* = 1.17/*d*(nm) × 100%, where *d* is particle diameter [26]. Inductively coupled plasma mass spectrometry (ICP-MS) measurements were performed with an Agilent ICP-MS 4500 instrument to measure the content of Au in each sample. Specific surface areas of the catalysts were measured by N<sub>2</sub> adsorption with Micromeritics Tristar II 3020.

CO<sub>2</sub> adsorption measurements were performed on a Micromeritics ASAP 2020 instrument. Typically, the sample loaded in a quartz tube was first pretreated with high-purity He at 423 K for 2 h. After the sample was cooled down to 323 K, the reactor was evacuated for 1 h. Then, CO<sub>2</sub> adsorption was performed by dosing certain amount of CO<sub>2</sub>. After adsorption for 30 min, the gas phase and the weakly adsorbed CO<sub>2</sub> were evacuated. Then, CO<sub>2</sub> adsorption amount was evaluated by the difference between the CO<sub>2</sub> amounts injected and evacuated.

The strength of basicity for different supports was estimated by Hammett titration. The methyl red, bromothymol blue, phenolphthalein, 2,4-dinitroaniline, and 4-nitroaniline were used as the Hammett indicators with the pK<sub>a</sub> values of +4.8, +7.2, +9.3, +15.0, and +18.4, respectively. The indicators were dissolved in petroleum ether of reagent grade and its concentration was ~0.1 wt%. After drying in vacuum, 100 mg of grinded sample was rapidly transferred into a tube and 1 mL of petroleum ether was injected to cover the sample. Subsequently, several drops of indicator solution were added followed by vigorous shaking. The strength of the basicity of supports was determined by the color change.

### 2.3. Catalytic reaction

The oxidative esterification of MAL and other aldehydes or alcohols to methyl esters was performed in a batch-type Teflon-lined stainless-steel autoclave. Typically, MAL purchased from Alfa Aesar (12 mmol) and the catalyst (typically, 0.50 g) were added into the reactor pre-charged with methanol (20 mL). After the introduction of O<sub>2</sub> with a certain pressure (typically 0.2 MPa), the mixture was heated up to a reaction temperature (typically 343 K) in an oil bath, and then the catalytic reaction was started by vigorously stirring. After a fixed time (typically 2 h, recorded as reaction time), the reaction was stopped by cooling down the reactor to room temperature in cold water. The products were analyzed by a gas chromatograph equipped with a FID detector and a capillary column (DB-FFAP, 60 m × 0.32 mm × 0.25 μm) using ethanol as an external standard for quantification.

## 3. Results and discussion

### 3.1. Catalytic behaviors of Au nanoparticles loaded on different supports

**Table 1** shows the catalytic performances of Au catalysts loaded on different supports for the direct oxidative esterification of MAL with methanol in the presence of O<sub>2</sub> to MMA. Au catalysts loaded on some metal oxides without basicity such as SiO<sub>2</sub>, TiO<sub>2</sub>, and SBA-15 showed poorer activity for the conversion of MAL. The selectivities of MMA over these catalysts were also quite lower. Many side reactions occurred over these catalysts, and the main by-products included isobutyric acid, isobutyl aldehyde, dimers of the methacrolein, and CO<sub>2</sub>. The employment of Al<sub>2</sub>O<sub>3</sub>, ZnO, ZrO<sub>2</sub>, and hydroxyapatite as the supports of Au catalysts provided moderate MMA selectivities (68–83%) although the conversions of MAL over these catalysts were not high. Among all of the catalysts examined in the present work, the Au/MgO and Au/hydrotalcite (HT) exhibited the best performance for the conversion of MAL to MMA; the yields of MMA were 97% and 90% over the Au/MgO and Au/HT, respectively.

**Table 1**  
Catalytic performances of Au catalysts loaded on different supports for the oxidative esterification of MAL with CH<sub>3</sub>OH in the presence of O<sub>2</sub>.<sup>a</sup>

Catalyst	MAL conv. (%)	Selectivity <sup>b</sup> (%)			
		MMA	MIB	MAA	Others
Au/SiO <sub>2</sub>	16	16	0.5	1.1	82
Au/SBA-15	13	8.8	0.3	0.8	90
Au/Al <sub>2</sub> O <sub>3</sub>	42	80	1.6	3.0	16
Au/TiO <sub>2</sub>	25	39	1.5	0.8	59
Au/ZrO <sub>2</sub>	33	67	0.2	0.2	33
Au/ZnO	28	78	2.7	0.1	19
Au/CeO <sub>2</sub>	58	99	0.3	0.3	0.4
Au/MgO	98	99	0.4	0.1	0.4
Au/HT	99	91	0.4	0.1	8.4
Au/HAP	31	83	0.6	0.2	16

<sup>a</sup> Reaction conditions: catalyst (Au loading, ~0.45 wt%), 0.50 g; CH<sub>3</sub>OH/MAL = 40:1 (molar ratio); CH<sub>3</sub>OH, 20 mL; P(O<sub>2</sub>) = 0.2 MPa; T = 343 K; t = 2 h.

<sup>b</sup> MMA, methyl methacrylate; MIB, methyl isobutyrate; MAA, methacrylic acid; others include isobutyric acid, isobutyl aldehyde, dimers of the methacrolein, CO<sub>2</sub>, and some unknown products.

**Table 2**

Properties of Au catalysts loaded on different supports.

Catalyst	Au content <sup>a</sup> (wt%)	Au particle size <sup>b</sup> (nm)	Surface area <sup>c</sup> (m <sup>2</sup> g <sup>-1</sup> )
Au/SiO <sub>2</sub>	0.43	2.2	180
Au/SBA-15	0.44	3.2	227
Au/Al <sub>2</sub> O <sub>3</sub>	0.43	2.5	104
Au/TiO <sub>2</sub>	0.45	2.3	22
Au/ZrO <sub>2</sub>	0.43	2.5	1.6
Au/ZnO	0.42	1.9	2.7
Au/CeO <sub>2</sub>	0.45	2.3	2.7
Au/MgO	0.45	2.2	14
Au/HT	0.45	2.5	13
Au/HAP	0.44	2.4	30

<sup>a</sup> Obtained from ICP-MS.<sup>b</sup> Evaluated from TEM.<sup>c</sup> Calculated from N<sub>2</sub> physisorption.

respectively, at 343 K after 2 h of reaction. The Au/CeO<sub>2</sub> catalyst also showed very high selectivity to MMA (99%), but the MAL conversion over this catalyst was inferior to those over the Au/MgO and Au/HT catalysts.

### 3.2. Characterizations of Au catalysts loaded on different supports and the effects of the support

The ICP-MS analysis showed that the Au content in each catalyst was approximately 0.45 wt% (Table 2), close to the target value (0.5 wt%) used in the preparation gel. Fig. 1 shows the TEM micrographs for some typical supported Au catalysts used in this work. From Fig. 1, it is clear that the Au particles are well dispersed on the supports in these catalysts. The mean sizes of the Au particles estimated by counting 150–200 particles over these catalysts were quite similar. As summarized in Table 2, the mean sizes of Au nanoparticles in all of the catalysts used in the present work

were also similar, ranging from 1.9 to 3.2 nm. These clearly suggest that the DP method using urea as a homogeneous precipitant is an effective technique to successfully deposit Au nanoparticles with similar sizes onto different supports. Thus, we speculate that the differences in the catalytic performances among the catalysts with different supports mainly arise from the property of the support.

The BET surface area for each catalyst is also displayed in Table 2. The Au/SBA-15 possesses the largest surface area, but this catalyst has shown very poor activity for the conversion of MAL (Table 1). The Au/TiO<sub>2</sub>, Au/MgO, and Au/HT catalysts possess moderate surface areas, but only the latter two catalysts are efficient for the oxidative esterification of MAL to MMA. This indicates that the BET surface area of the catalyst is not a key factor influencing the catalytic performances.

The Hammett titration method can be used to determine the strength of acidity and basicity for solid acids and solid bases [27]. The change in color of an indicator in the suspension containing a solid base indicates that the Hammett value (basicity) of this base was higher than the pK<sub>a</sub> of the indicator. Table 3 displays the results obtained from the Hammett titration for different supports. Among all the supports, only MgO and HT could induce a color change for phenolphthalein (pK<sub>a</sub> = 9.3), indicating that these two supports possess stronger basic sites. The titration results also suggest that the strength of basicity decreases in the order of MgO, HT > HAP, Al<sub>2</sub>O<sub>3</sub> > CeO<sub>2</sub>, ZnO > ZrO<sub>2</sub>, TiO<sub>2</sub>, SiO<sub>2</sub> and SBA-15. MgO- and HT-supported Au catalysts were the most efficient catalysts for the conversion of MAL to MMA, while the use of SiO<sub>2</sub>, SBA-15, or TiO<sub>2</sub> as the support provided much poorer catalytic performances (Table 1). This may suggest that the strength of the basicity of the support plays a role in the oxidative esterification reaction.

We also quantified the density of basic sites on each support by measuring the adsorption amount of CO<sub>2</sub>. As displayed in Table 4, Al<sub>2</sub>O<sub>3</sub>, MgO, HT, and HAP are capable of adsorbing larger amounts of CO<sub>2</sub> per gram of catalysts. In contrast, no adsorption of CO<sub>2</sub> was

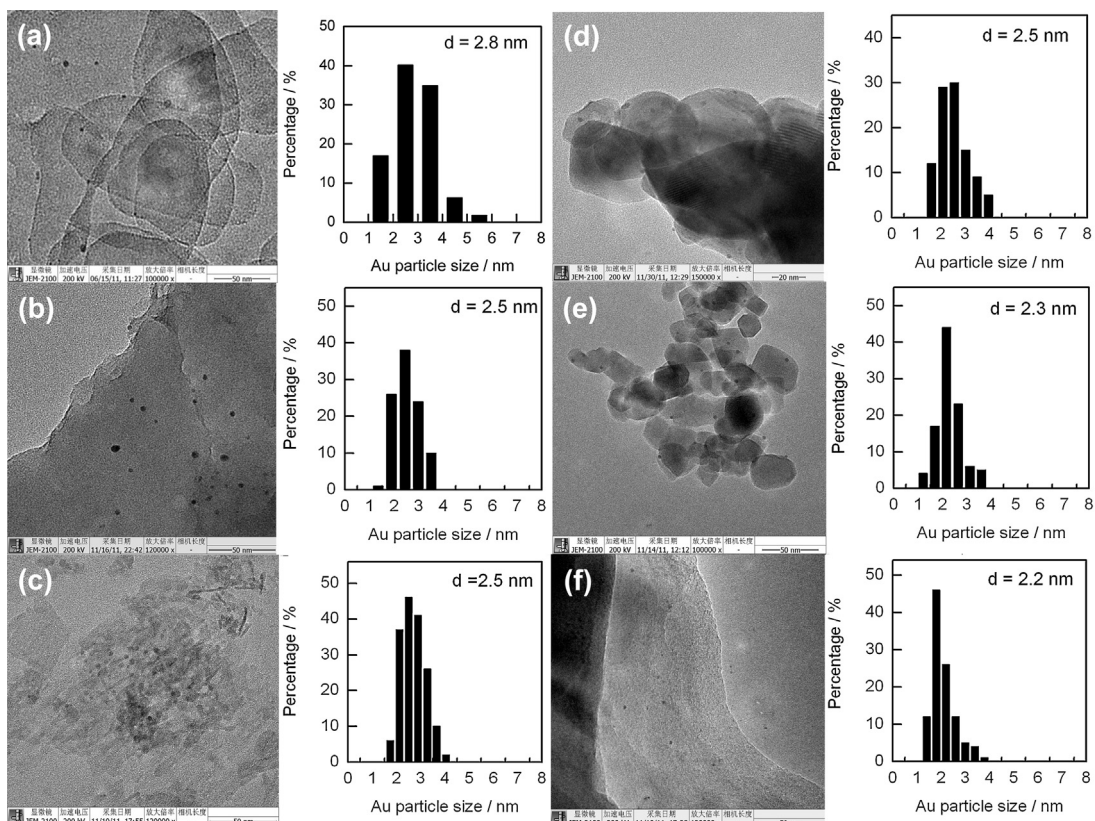


Fig. 1. TEM micrographs of Au nanoparticles loaded on different supports. (a) MgO, (b) HT, (c) Al<sub>2</sub>O<sub>3</sub>, (d) ZrO<sub>2</sub>, (e) TiO<sub>2</sub>, and (f) SiO<sub>2</sub>.

**Table 3**

Results obtained from the Hammett titration with various indicators for different supports.

Support	Indicators ( $pK_a$ )				
	Methyl red (4.8)	Bromothymol blue (7.2)	Phenolphthalein (9.3)	2,4-Dinitro-aniline (15.0)	4-Nitroaniline (18.4)
MgO	+	+	+	–	–
HT	+	+	+	–	–
$\gamma\text{-Al}_2\text{O}_3$	+	+	–	–	–
HAP	+	+	–	–	–
CeO <sub>2</sub>	+	–	–	–	–
ZnO	+	–	–	–	–
TiO <sub>2</sub>	–	–	–	–	–
ZrO <sub>2</sub>	–	–	–	–	–
SiO <sub>2</sub>	–	–	–	–	–
SBA-15	–	–	–	–	–

+, color change occurs; –, no color change occurs.

**Table 4**

The adsorption amounts of CO<sub>2</sub> over different supports.

Support	CO <sub>2</sub> adsorption amount	
	Per gram ( $\mu\text{mol g}^{-1}$ )	Per surface area ( $\mu\text{mol m}^{-2}$ )
MgO	44.0	3.2
HT	43.5	3.4
CeO <sub>2</sub>	3.9	1.4
Al <sub>2</sub> O <sub>3</sub>	80.1	0.8
HAP	41.8	1.4
ZnO	3.3	1.2
ZrO <sub>2</sub>	10.9	0.9
TiO <sub>2</sub>	1.2	0.1
SiO <sub>2</sub>	0	0
SBA-15	0	0

observed over SBA-15 and SiO<sub>2</sub>, indicating the absence of basic sites over these two supports. Medium to lower adsorption amounts of CO<sub>2</sub> were observed over ZrO<sub>2</sub>, CeO<sub>2</sub>, ZnO, and TiO<sub>2</sub>, by taking account into the surface area, the density of basic sites per surface area was also evaluated. Among all the supports, MgO and HT bearing stronger basicity also showed the highest densities of basic sites. CeO<sub>2</sub>, HAP, ZnO, ZrO<sub>2</sub>, and Al<sub>2</sub>O<sub>3</sub> possessed medium densities of basic sites, whereas TiO<sub>2</sub> possessed a lower density of basic sites. This trend correlates well with that for the change of catalytic performance by changing the support (Table 1). These results allow us to propose that the basicity of support plays key roles in the oxidative esterification of MAL with CH<sub>3</sub>OH to MMA.

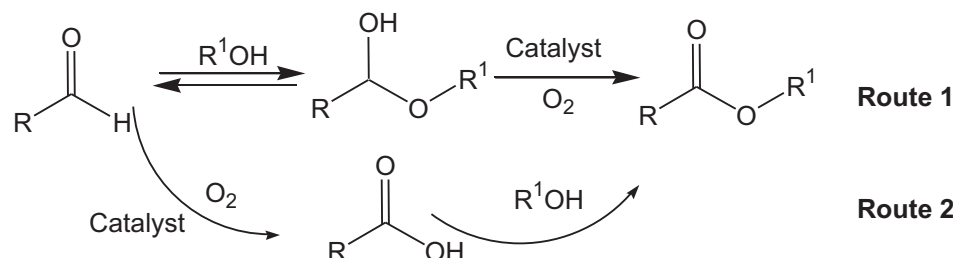
Recently, several groups have investigated the reaction mechanism for the oxidative esterification of aldehydes with alcohols over both Pd- and Au-based catalysts [6,19,28]. The reaction has been proposed to proceed through the initial formation of a hemiacetal intermediate, followed by the oxidation of the hemiacetal to ester (Scheme 2, route 1). The oxidation of aldehyde to carboxylic acid in the first step followed by the esterification of carboxylic acid with alcohol to ester in the second step may also be possible (Scheme 2, route 2). In our case, we could not observe the formation of significant amount of methacrylic acid (MAA), a direct oxidative

product from MAL conversion, during the whole reaction process. In addition, the leaching of MgO, which might have been caused by the reaction with MAA, an acid, if it is formed during the reaction, has not occurred. Thus, we speculate that the reaction over our Au/MgO catalyst may proceed via route 1 in Scheme 2. It has been reported that the presence of a base can accelerate the formation of hemiacetal [29] and is also essential for the consecutive oxidation of the intermediate [13]. Therefore, for the oxidative esterification of MAL, it is understandable that MgO or HT-supported catalyst containing high density of basic sites, particularly the stronger basic sites, favors the formation of MMA.

### 3.3. Effect of size of Au nanoparticles over Au/MgO catalysts

It is well known that the size of Au nanoparticles significantly affects their catalytic behaviors in many reactions [7–11,30–32]. By regulating the concentration of Au precursor ([HAuCl<sub>4</sub>]), the aging time, and the calcination conditions used in the catalyst preparation by the DP method, we have succeeded in preparing the MgO-supported Au catalysts containing Au nanoparticles with mean sizes ranging from 2.2 to 10 nm. Table 5 shows the conditions used in the preparation and the corresponding mean sizes of Au nanoparticles derived from TEM in the final catalysts after H<sub>2</sub> reduction. Typical TEM micrographs and the Au particle size distributions for these catalysts are shown in Fig. 2. Table 5 shows that the increase in the concentration of HAuCl<sub>4</sub> decreases the mean size of Au nanoparticles. The prolonging of aging time also significantly increased the size of Au nanoparticles probably due to the Ostwald ripening, which was caused by the dissolved smaller particles precipitating onto the larger particles [25].

We have investigated the catalytic performances of the Au/MgO catalysts with different mean sizes of Au nanoparticles for the oxidative esterification of MAL with CH<sub>3</sub>OH in the presence of O<sub>2</sub>. Table 6 shows the results obtained at 343 K after 2 h of reaction. Without Au, no formation of MMA was observed. After the loading of Au particles, the conversion of MAL increased significantly, and MMA was formed as a major product, suggesting that the Au

**Scheme 2.** Possible mechanism for oxidative esterification of aldehydes to esters.

**Table 5**

Effect of preparation conditions on the mean size and dispersion of Au nanoparticles over Au/MgO catalysts.

Entry	[HAuCl <sub>4</sub> ] (mol/L)	Aging time (h)	Mean Au size <sup>a</sup> (nm)	Au dispersion <sup>b</sup> (%)
1	0.96	4	2.2	53
2	0.48	4	2.8	42
3	0.24	4	3.5	33
4	0.12	4	4.1	29
5	0.12	8	5.0	23
6	0.12	16	6.1	19
7 <sup>c</sup>	0.12	16	10	12

<sup>a</sup> Obtained from TEM.

<sup>b</sup> Estimated from the mean size of Au.

<sup>c</sup> The sample was calcined in air at 673 K for 2 h.

nanoparticles accelerated the conversion of MAL and were crucial for the formation of MMA. The catalyst with smaller Au nanoparticles provided higher MAL conversion. To gain further insights into the Au particle size effect, we have performed the conversion of MAL at short reaction time over the Au/MgO catalysts with different mean sizes of Au nanoparticles. We measured the MAL conversions at the initial reaction stage for these catalysts and evaluated the initial rate of MAL conversion by using the slopes of the straight lines obtained in the plots of the conversion versus reaction time (Fig. 3). The initial rate of MAL conversion increased markedly as the size of the Au particles decreased from 10 nm to 2.2 nm (Table 7). The selectivity of MMA was >93% over each catalyst under these conditions. We have also calculated the turnover frequency (TOF), i.e., the moles of MAL converted per unit time at the initial stage per mole of surface Au atoms. The catalysts with smaller Au nanoparticles exhibit higher TOFs for the conversion of

MAL (Fig. 4). Our results suggest that the oxidative esterification of MAL with methanol over the Au/MgO catalyst is a structure-sensitive reaction. The facile activation of O<sub>2</sub> or the intermediate may be the reason for the higher TOFs over the smaller Au nanoparticles, which contains higher fraction of coordinatively unsaturated Au sites [25].

### 3.4. Optimization of Au loading, recycling uses and substrate scope of Au/MgO catalyst

The results described above suggest that the basicity and the Au particle size are two crucial factors determining the catalytic behaviors of the supported Au nanoparticles for the oxidative esterification of MAL with methanol in the presence of O<sub>2</sub> under liquid base-free conditions. The Au/MgO with strong basicity and a mean

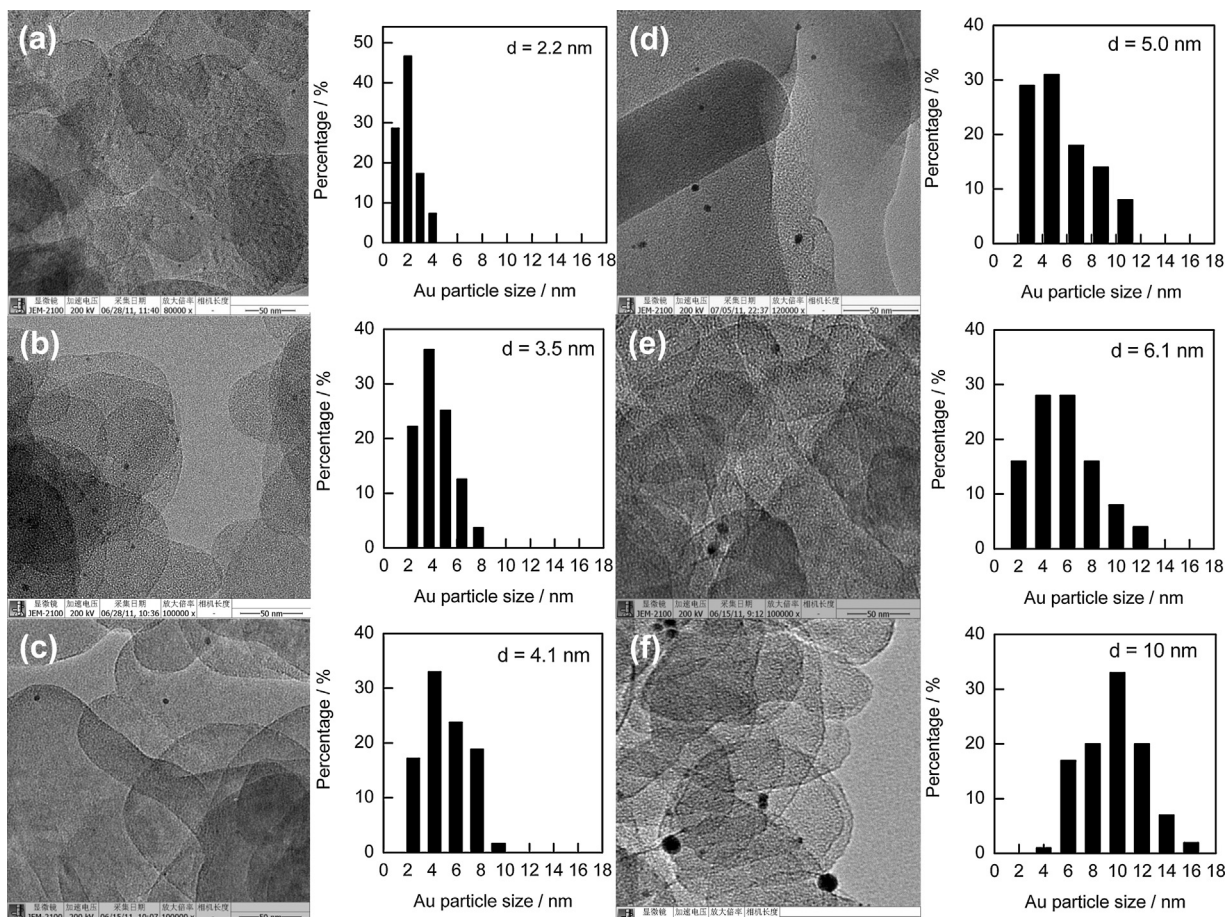


**Fig. 2.** TEM micrographs of Au/MgO catalysts prepared under different conditions and the corresponding particle size distributions. The conditions are displayed in Table 5; the conditions used for the preparation of samples (a), (b), (c), (d), (e), and (f) correspond to Entries of 1, 3, 4, 5, 6, and 7 in Table 5, respectively.

**Table 6**

Catalytic performances of MgO-supported Au nanoparticles with different mean sizes for oxidative esterification of MAL with  $\text{CH}_3\text{OH}$  in the presence of  $\text{O}_2$ .<sup>a</sup>

Catalyst	MAL conv. (%)	Selectivity <sup>b</sup> (%)			
		MMA	MIB	MAA	Others
MgO	1.7	0	0	0	1.7
Au/MgO (Au, 2.8 nm)	62	98	0.4	0	1.6
Au/MgO (Au, 3.5 nm)	57	98	0.6	0	1.4
Au/MgO (Au, 4.1 nm)	44	97	0.6	0	2.4
Au/MgO (Au, 6.2 nm)	19	93	0.3	0.1	6.7

<sup>a</sup> Reaction conditions: catalyst (Au loading 0.45 wt%) = 0.30 g;  $\text{CH}_3\text{OH}:\text{MAL}$  = 40:1 (molar ratio);  $\text{CH}_3\text{OH}$ , 20 mL;  $P(\text{O}_2)$  = 0.2 MPa;  $T$  = 343 K;  $t$  = 2 h.

<sup>b</sup> MMA, methyl methacrylate; MIB, methyl isobutyrate; MAA, methacrylic acid; others includes isobutyric acid, isobutyl aldehyde, dimers of the methacrolein,  $\text{CO}_2$  and other unknown products.

**Table 7**

Effect of the mean size of Au nanoparticles on the initial rate of MAL conversion.

Mean Au size (nm)	Initial MAL conversion rate ( $\mu\text{mol g}^{-1} \text{s}^{-1}$ )
2.2	5.6
3.5	3.1
4.1	2.2
6.2	1.1
10.0	0.55

Reaction conditions: catalyst (Au loading 0.45 wt%) = 0.30 g;  $\text{CH}_3\text{OH}:\text{MAL}$  = 40:1 (molar ratio);  $\text{CH}_3\text{OH}$ , 20 mL;  $P(\text{O}_2)$  = 0.2 MPa;  $T$  = 343 K.

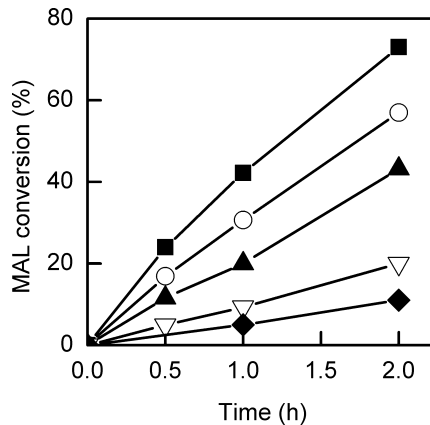


**Fig. 3.** Catalytic performances of Au/MgO catalysts with different mean sizes of Au particles for oxidative esterification of MAL. Reaction conditions: catalyst (Au loading 0.45 wt%), 0.30 g;  $\text{CH}_3\text{OH}:\text{MAL}$  = 40:1 (molar ratio);  $\text{CH}_3\text{OH}$ , 20 mL;  $P(\text{O}_2)$  = 0.2 MPa;  $T$  = 343 K.

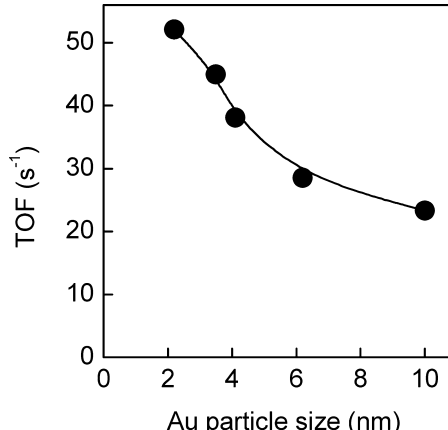


**Fig. 4.** Dependence of TOF for MAL conversion over Au/MgO catalysts on the mean size of Au particles. Reaction conditions: catalyst (Au loading, 0.45 wt%) = 0.30 g;  $\text{CH}_3\text{OH}:\text{MAL}$  = 40:1 (molar ratio);  $\text{CH}_3\text{OH}$ , 20 mL;  $P(\text{O}_2)$  = 0.2 MPa;  $T$  = 343 K.

**Table 8**

Effect of Au loadings on catalytic performances of Au/MgO catalysts for oxidative esterification of MAL with  $\text{CH}_3\text{OH}$  in the presence of  $\text{O}_2$ .<sup>a</sup>

Au loadings (wt%)	MAL conv. (%)	Selectivity <sup>b</sup> (%)			
		MMA	MIB	MAA	Others
0	1.7	0	0	0	1.7
0.11	30	98	0.7	0.2	1.2
0.25	65	98	0.6	0.2	1.2
0.36	86	99	0.5	0.1	0.3
0.45	98	99	0.4	0.1	0.4
0.55	100	>99	0.2	0	0.3

<sup>a</sup> Reaction conditions: Au/MgO, 0.50 g;  $\text{CH}_3\text{OH}:\text{MAL}$  = 40:1 (molar ratio);  $\text{CH}_3\text{OH}$ , 20 mL;  $P(\text{O}_2)$  = 0.2 MPa;  $T$  = 343 K;  $t$  = 2 h.

<sup>b</sup> MMA, methyl methacrylate; MIB, methyl isobutyrate; MAA, methacrylic acid; others includes isobutyric acid, isobutyl aldehyde, dimers of the methacrolein,  $\text{CO}_2$  and other unknown products.

Au particle size of 2.2 nm could afford a MMA yield of 98% at 343 K after 2 h of reaction.

We have investigated the effect of the loading amount of Au on catalytic performances for the oxidative esterification of MAL with methanol. As shown in Table 8, in the absence of Au the conversion of MAL was very low (1.7%) and no formation of MMA was observed. After the loading of a small amount of Au particles onto MgO, the conversion of MAL increased remarkably, and MMA was formed as a major product. The increase in the Au loading led to an increase in the MAL conversion. A high yield of MMA (>95%) could be attained as Au loading was  $\geq 0.45$  wt%. These results provide further evidence that the Au nanoparticles accelerate the conversion of MAL and are responsible for the formation of MMA. Taking the MMA yield and the cost of catalyst into consideration, it is clear that the Au loading of 0.45 wt% is appropriate for the oxidative esterification of MAL with methanol to MMA.

Besides the yield of MMA, the stability of the catalyst is also a key factor for its practical application. Thus, we performed the recycling uses of the Au/MgO catalyst with an Au loading of 0.45 wt% for the oxidative esterification of MAL with methanol. After each run, the catalyst was recovered by filtration, washing and drying, and then was re-used in the next run. Fig. 5 shows that the MAL conversion decreased only slightly in the initial 4 recycles, and then kept almost unchanged in the 5th recycle. Meanwhile, the selectivity to MMA was kept as high as 99%. After 5 recycles, the MAL conversion and the MMA yield could still be sustained at >90%. This indicates that the Au/MgO catalyst is stable during the recycling uses for the conversion of MAL with methanol in the presence of  $\text{O}_2$ .

We have also examined the catalytic performances of the Au/MgO (Au, 2.2 nm) catalyst for the liquid base-free oxidative

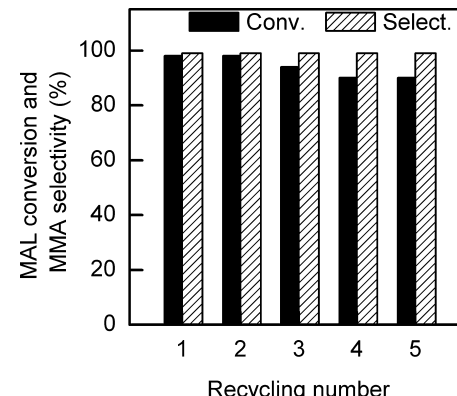


**Fig. 5.** Recycling uses of Au/MgO catalyst for oxidative esterification of MAL. Reaction conditions: catalyst (Au loading, 0.45 wt%) = 0.50 g;  $\text{CH}_3\text{OH}:\text{MAL}$  = 40:1 (molar ratio);  $\text{CH}_3\text{OH}$ , 20 mL;  $P(\text{O}_2)$  = 0.2 MPa;  $T$  = 343 K;  $t$  = 2 h.

**Table 9**Oxidative esterification of various substrates with methanol over the Au/MgO catalyst.<sup>a</sup>

Entry	Reactant	Product	Reaction time (h)	Conv. (%)	Select. (%)
1			3	99	87
2			3	65	92
3			3	96	>99
4			6	94	92
5			6	>99	97
6			12	81	80
7			6	12	66
8			3	39	97
9			12	89	98

Reaction conditions: catalyst (Au loading, 0.45 wt%) = 0.50 g; CH<sub>3</sub>OH:substrate = 40:1 (molar ratio); CH<sub>3</sub>OH, 20 mL; P(O<sub>2</sub>) = 0.5 MPa; T = 353 K.

esterification of a wide scope of aldehydes and alcohols with methanol under O<sub>2</sub> atmosphere. As shown in Table 9, the conversion of benzaldehyde to methyl benzoate could be catalyzed by the Au/MgO catalyst at 353 K with a good efficiency and the yield of methyl benzoate reached ~87% (Entry 1). Benzyl alcohol could also be selectively transformed to methyl benzoate although the conversion was relatively low (Entry 2). Notably, o- and p-methoxy benzyl alcohols and p-methyl benzyl alcohol could facilely be converted to the corresponding methyl esters in high yields under appropriate reaction conditions (Entries 3–5). The conversions of 4-(trifluoromethyl)benzyl alcohol to the corresponding methyl esters (Entry 7) became difficult. The conversion of octanol, an aliphatic

alcohol, increased from 39% to 89% with prolonging the reaction time from 3 to 12 h over the Au/MgO catalyst, while the selectivity of methyl octanate kept at 97–98% at the same time. Thus, the present Au/MgO catalyst favors the oxidative esterification of benzylic alcohols containing electron-donating groups to the corresponding methyl esters, while it is difficult for the conversion of benzylic alcohols containing electron-withdrawing groups.

#### 4. Conclusions

The comparison among Au catalysts loaded on a series of supports reveals that the support plays significant roles in determining

both the activity and selectivity for the oxidative esterification of MAL to MMA under liquid base-free conditions. We have clearly demonstrated that the support with a larger density of basic sites (particularly stronger basic site) provides a higher yield of MMA. The basic site has been proposed to accelerate the formation of hemiacetal intermediate and thus contributes to enhancing the formation of MMA. The size of Au nanoparticles is another key factor strongly influencing the catalytic activity. The smaller Au nanoparticles exhibit higher conversions of MAL. We have clarified that the TOF for MAL conversion depends on the mean size of Au particles loaded on MgO, and the decrease in the mean size of Au particles in a range of 10–2.2 nm increases the TOF. This indicates that the Au-catalyzed oxidative esterification of MAL is a structure-sensitive reaction. Over the Au/MgO catalyst with a mean size of Au particles of 2.2 nm, 98% MAL conversion and 99% MMA selectivity have been achieved at 343 K after 2 h of reaction. The catalyst is stable and can be used recyclably without significant deactivation. The Au/MgO catalyst is also applicable to the oxidative esterification of benzaldehyde, benzylic alcohols and aliphatic alcohols under liquid base-free conditions.

## Acknowledgements

This work was supported by the National Basic Program of China (Nos. 2010CB732303 and 2013CB933100) and the Program for Changjiang Scholars and Innovative Research Team in University (No. IRT1036).

## References

- [1] K. Nagai, Appl. Catal. A: Gen. 221 (2001) 367–377.
- [2] S. Yamamoto, T. Yamaguchi, K. Yokota, O. Nagano, M. Chono, A. Aoshima, Catal. Surv. Asia 14 (2010) 124–131.
- [3] C. Liu, J. Wang, L. Meng, Y. Deng, Y. Li, A. Lei, Angew. Chem. Int. Ed. 50 (2011) 5144–5148.
- [4] B. Wang, W. Ran, W. Sun, K. Wang, Ind. Eng. Chem. Res. 51 (2012) 3932–3938.
- [5] B. Wang, W. Sun, J. Zhu, W. Ran, S. Chen, Ind. Eng. Chem. Res. 51 (2012) 15004–15010.
- [6] Y. Diao, R. Yan, S. Zhang, P. Yang, Z. Li, L. Wang, H. Dong, J. Mol. Catal. A 303 (2009) 35–42.
- [7] A.S.K. Hashimi, G.J. Hutchings, Angew. Chem. Int. Ed. 45 (2006) 7896–7936.
- [8] C.D. Pina, E. Falletta, L. Prati, M. Rossi, Chem. Soc. Rev. 37 (2008) 2077–2095.
- [9] A. Corma, H. Garcia, Chem. Soc. Rev. 37 (2008) 2096–2126.
- [10] Y. Zhang, X. Cui, F. Shi, Y. Deng, Chem. Rev. 112 (2012) 2467–2505.
- [11] T. Takei, T. Akita, I. Nakamura, T. Fujitani, M. Okumura, K. Okazaki, J. Huang, T. Ishida, M. Haruta, Adv. Catal. 55 (2012) 1–126.
- [12] T. Hayashi, T. Inagaki, N. Itayama, H. Baba, Catal. Today 117 (2006) 210–213.
- [13] I.S. Nielsen, E. Taarning, K. Egeblad, R. Madsen, C.H. Christensen, Catal. Lett. 116 (2007) 35–40.
- [14] E. Taarning, A.T. Madsen, J.M. Marchetti, K. Egeblad, C.H. Christensen, Green Chem. 10 (2008) 408–414.
- [15] G.L. Brett, P.J. Miedziak, N. Dimitratos, J.A. Lopez-Sanchez, N.F. Dummer, R. Tiruvallam, C.J. Kiely, D.W. Knight, S.H. Taylor, D.J. Morgan, A.F. Carley, G.J. Hutchings, Catal. Sci. Technol. 2 (2012) 97–104.
- [16] O. Casanova, S. Iborra, A. Corma, J. Catal. 265 (2009) 109–116.
- [17] X. Wang, G. Zhao, H. Zou, Y. Cao, Y. Zhang, R. Zhang, F. Zhang, M. Xian, Green Chem. 13 (2011) 2690–2695.
- [18] T. Ishida, M. Nagaoka, T. Akita, M. Haruta, Chem. Eur. J. 14 (2008) 8456–8460.
- [19] F. Su, J. Ni, H. Sun, Y. Cao, H. He, K. Fan, Chem. Eur. J. 14 (2008) 7131–7135.
- [20] R.L. Oliveira, P.K. Kiyohara, L.M. Rossi, Green Chem. 11 (2009) 1366–1370.
- [21] L.A. Parreira, N. Bogdanchi-kova, A. Pestryakov, T.A. Zepeda, I. Tuzovskaya, M.H. Farias, E.V. Gusevskaya, Appl. Catal. A 397 (2011) 145–152.
- [22] Y. Hao, Y. Chong, S. Li, H. Yang, J. Phys. Chem. C 116 (2012) 6512–6519.
- [23] H. Miyamura, T. Yasukawa, S. Kobayashi, Green Chem. 12 (2010) 776–778.
- [24] P. Liu, C. Li, J.M. Hensen, Chem. Eur. J. 18 (2012) 12122–12129.
- [25] W. Fang, J. Chen, Q. Zhang, Y. Wang, Chem. Eur. J. 17 (2011) 1247–1256.
- [26] G.C. Bond, D.T. Thompson, Catal. Rev. Sci. Eng. 41 (1999) 319–388.
- [27] Z. Yang, Y. Li, Q. Wu, N. Ren, Y. Zhang, Z. Liu, Y. Tang, J. Catal. 280 (2011) 247–254.
- [28] K. Suzuki, T. Yamaguchi, K. Matsushita, C. Iitsuka, J. Miura, T. Akaogi, H. Ishida, ACS Catal. 3 (2013) 1845–1849.
- [29] S. Kiyooka, Y. Wada, M. Ueno, T. Yokoyama, R. Yokoyama, Tetrahedron 63 (2007) 12695–12701.
- [30] M. Haruta, Gold Bull. 37 (2004) 27–36.
- [31] B. Hvolbæk, T.V.W. Janssens, B.S. Clausen, H. Falsig, C.H. Christensen, J.K. Nørskov, Nano Today 2 (2007) 14–18.
- [32] Q. Zhang, W. Deng, Y. Wang, Chem. Commun. 47 (2011) 9275–9292.